Chemical Science

ROYAL SOCIETY OF CHEMISTRY

EDGE ARTICLE

View Article Online
View Journal | View Issue

Cite this: *Chem. Sci.*, 2020, **11**, 5790

All publication charges for this article have been paid for by the Royal Society of Chemistry

Carboxylate breaks the arene C–H bond *via* a hydrogen-atom-transfer mechanism in electrochemical cobalt catalysis†

Xin-Ran Chen,[a] Shuo-Qing Zhang,[a] Tjark H. Meyer,[b] Chun-Hui Yang,[d] Qin-Hao Zhang,[a] Ji-Ren Liu,[a] Hua-Jian Xu,*[d] Fa-He Cao,*[c] Lutz Ackermann*[b] and Xin Hong*[a]

Combined computational and experimental studies elucidated the distinctive mechanistic features of electrochemical cobalt-catalyzed C–H oxygenation. A sequential electrochemical–chemical (EC) process was identified for the formation of an amidylcobalt(III) intermediate. The synthesis, characterization, cyclic voltammetry studies, and stoichiometric reactions of the related amidylcobalt(III) intermediate suggested that a second on-cycle electro-oxidation occurs on the amidylcobalt(III) species, which leads to a formal Co(IV) intermediate. This amidylcobalt(IV) intermediate is essentially a cobalt(III) complex with one additional single electron distributed on the coordinating heteroatoms. The radical nature of the coordinating pivalate allows the formal Co(IV) intermediate to undergo a novel carboxylate-assisted HAT mechanism to cleave the arene C–H bond, and a CMD mechanism could be excluded for a Co(III/I) catalytic scenario. The mechanistic understanding of electrochemical cobalt-catalyzed C–H bond activation highlights the multi-tasking electro-oxidation and the underexplored reaction channels in electrochemical transition metal catalysis.

Received 2nd April 2020
Accepted 19th May 2020

DOI: 10.1039/d0sc01898h

rsc.li/chemical-science

Introduction

Due to the remarkable availability and sustainability of electricity, electrochemical C–H bond activation and functionalization has recently emerged as a powerful approach of green synthesis.[1] The merging of electrochemical C–H bond activation and 3d transition metal catalysis has successfully realized a series of electrochemical cobalt-catalyzed C–H bond transformations,[2] including C–H oxygenation[3] (Scheme 1a) and C–H amination[4] (Scheme 1b), as well as C–H/N–H annulation[5] (Scheme 1c) and carbonylation[6] (Scheme 1d). These transformations avoid stoichiometric oxidants, presenting an appealing synthetic strategy with exceptional resource-economy.

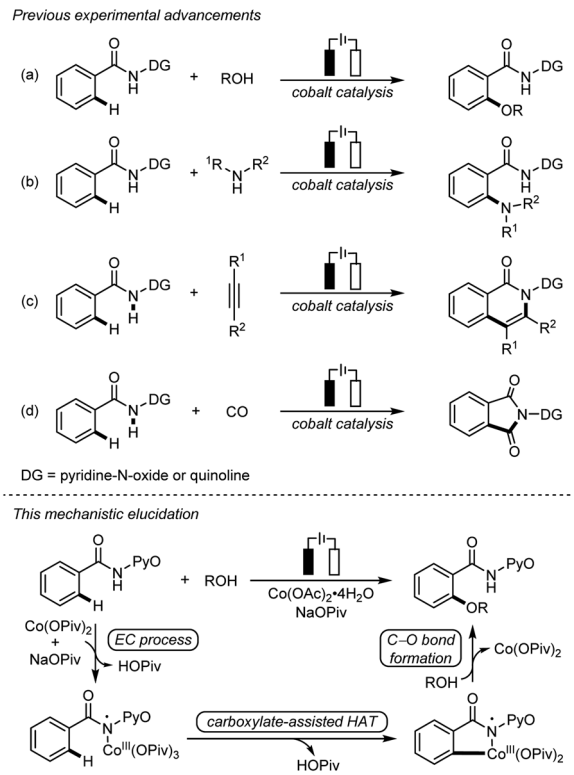

Scheme 1 Electrochemical cobalt-catalyzed C–H oxygenation.

[a]*Department of Chemistry, Zhejiang University, Hangzhou, 310027, China. E-mail: hxchem@zju.edu.cn*

[b]*Institut für Organische und Biomolekulare Chemie, Georg-August-Universität Göttingen, Tammannstraße 2, 37077 Göttingen, Germany. E-mail: Lutz.Ackermann@chemie.uni-goettingen.de*

[c]*School of Materials, Sun Yat-sen University, Guangzhou, 510006, China. E-mail: caofh5@mail.sysu.edu.cn*

[d]*School of Food and Biological Engineering, Hefei University of Technology, Hefei, 230009, China. E-mail: hjxu@hfut.edu.cn*

† Electronic supplementary information (ESI) available. CCDC 1969391. For ESI and crystallographic data in CIF or other electronic format see DOI: 10.1039/d0sc01898h

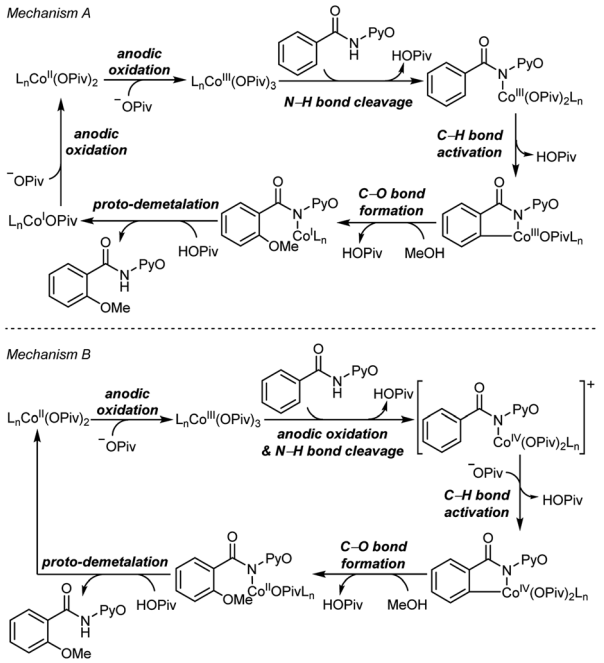

Scheme 2 Proposed catalytic cycles of electrochemical cobalt-catalyzed C–H oxygenation.

Despite the rich history and fruitful advances in the mechanistic studies on transition metal-catalyzed C–H bond activation,[7] the mechanistic understanding of electrochemical C–H bond activation still remains primitive.[8] Currently, little molecular-level understanding and controlling factors of electrochemical transition metal-catalyzed C–H bond activations are available, which presents a significant challenge for rational reaction design in this field. Herein, we report a mechanistic elucidation on electrochemical cobalt-catalyzed C–H oxygenation with combined computational and experimental studies (Scheme 1). A key electrochemical–chemical (EC) process was identified for the generation of amidylcobalt(III) species, based on density functional theory (DFT) calculations, cyclic voltammetry studies, characterization and stoichiometric transformations of the proposed amidylcobalt(III) species which allows a novel carboxylate-assisted HAT mechanism to cleave the arene C–H bond. These mechanistic features highlight the distinctive reaction channels in electrochemical transition metal catalysis, providing the molecular basis for rational reaction design in this field.

Results and discussion

Two mechanisms were proposed for electrochemical cobalt-catalyzed C–H functionalization (Scheme 2).[3–6,9] Mechanism A is a Co(III)–Co(I) catalytic cycle. It involves initial anodic oxidation of Co(II)pivalate to the corresponding Co(III) species. Subsequent N–H cleavage leads to the amidylcobalt(III) intermediate. This intermediate undergoes C–H bond activation, and subsequent C–O bond formation *via* the arylcobalt(III) species leads to the amidylcobalt(I) intermediate. Further proto-demetalation produces the oxygenated product and regenerates the cobalt catalyst. Mechanism B is a Co(IV)–Co(II) catalytic cycle. From the Co(III)pivalate, an anodic oxidation and N–H cleavage lead to the cationic amidylcobalt(IV) intermediate. This intermediate undergoes similar C–H bond activation, C–O bond formation and proto-demetalation to produce the oxgenated product.

The DFT-computed free energy changes of mechanism A and the oxidation potential of the involved intermediates are shown in Fig. 1.[10] The exergonic complexation of the quintet model complex $Co(OPiv)_3$ with amide substrate **1** leads to the quintet **int2**. This intermediate undergoes a facile carboxylate-assisted N–H cleavage *via* **TS3**, generating the amidylcobalt(III) intermediate **int4**. A subsequent carboxylate-assisted metalation process cleaves the arene C–H bond through **TS5** and generates

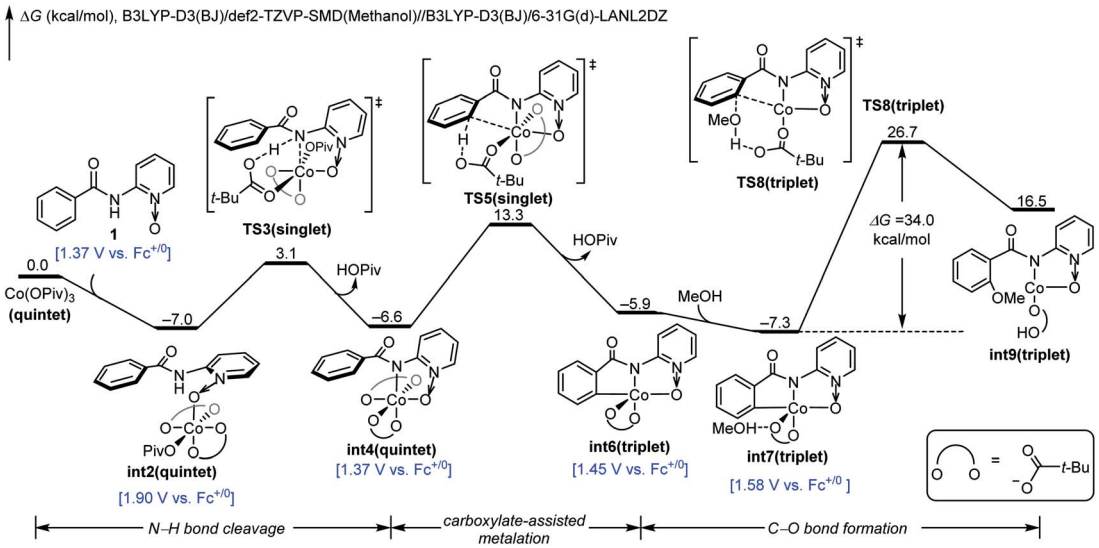

Fig. 1 DFT-computed free energy changes of mechanism A and computed oxidation potentials of intermediates before C–O bond formation.

the arylcobalt(III) intermediate **int6**. **int6** further complexes with methanol through hydrogen-bonding to form **int7**.

From **int7**, the C–O bond formation *via* **TS8** requires an unsurmountable barrier of 34.0 kcal mol^{-1}. We also considered the C–O bond formation process *via* reductive elimination of arylcobalt(III)(OMe) species, and this alternative process is even less favourable (Fig. S1†). Therefore, mechanism A is not operative due to the high C–O bond formation barrier of the arylcobalt(III) intermediate for the room-temperature catalytic C–H oxygenation. Only the most stable spin states are presented in Fig. 1; the detailed free energy profile with minimum-energy crossing point information and IRC confirmations of each transition state are included in the ESI (Fig. S2–S6†).

Our above computations suggest that the oxidation of Co(III) species prior to C–O bond formation is necessary. Based on the computed oxidation potentials of the involved organocobalt intermediates (Fig. 1), the amide substrate **1** and amidylcobalt(III) intermediate **int4** have the lowest oxidation potentials. These two species have the same oxidation potentials because the oxidation of **int4** mainly occurs on the coordinating amidyl fragment (Fig. S7†). The oxidation of **int4** leads to a Co(III) complex with a coordinating amidyl radical, a formal Co(IV) species **int10** (Fig. 2). If the electrochemical oxidation occurs on **int4**, Co(IV) generation involves sequential electrochemical oxidation of Co(II) pivalate and a chemical process (EC process, Fig. 2). Alternatively, the electrochemical oxidation of the amide substrate leads to two independent electrochemical oxidations (EE process, Fig. 2).[11]

The EC process can be identified by varying the scan rate in the cyclic voltammetry (CV) study.[11] The mixture of $Co(OAc)_2 \cdot 4H_2O$, $NaOPiv \cdot H_2O$ and amide **1** at a scan rate of 0.01 V s^{-1} showed an oxidation peak which corresponds to the oxidation of Co(II) to Co(III).[12] No reduction peak was identified at this slow scan rate, suggesting that the oxidized Co(III) species underwent a chemical transformation and the reduction of Co(III) did not occur. With increasing scan rate, the rate of the chemical transformation did not match the fast scan rate, and a reduction peak appeared (0.05 V s^{-1} and 1.00 V s^{-1}). CV studies with additional scan rates are included in the ESI (Fig. S16†). This observation is strongly suggestive of an EC process, and the key chemical process has a number of possibilities, including the coordination of the amide substrate, or the amide N–H bond cleavage.

The preparation, characterization and stoichiometric transformations of the proposed amidylcobalt(III) species revealed that the key chemical transformation that connects the two electro-oxidations is the amide N–H bond cleavage. The proposed amidylcobalt(III) species **A** was synthesized by reacting the amide substrate **1** with cobalt triacetoacetate, in the presence of silver acetate and sodium pivalate hydrate in chloroform (Scheme 3a). By the ESI-MS study of the synthesized **A**, a consistent molecular weight was found (Scheme 3a), and the

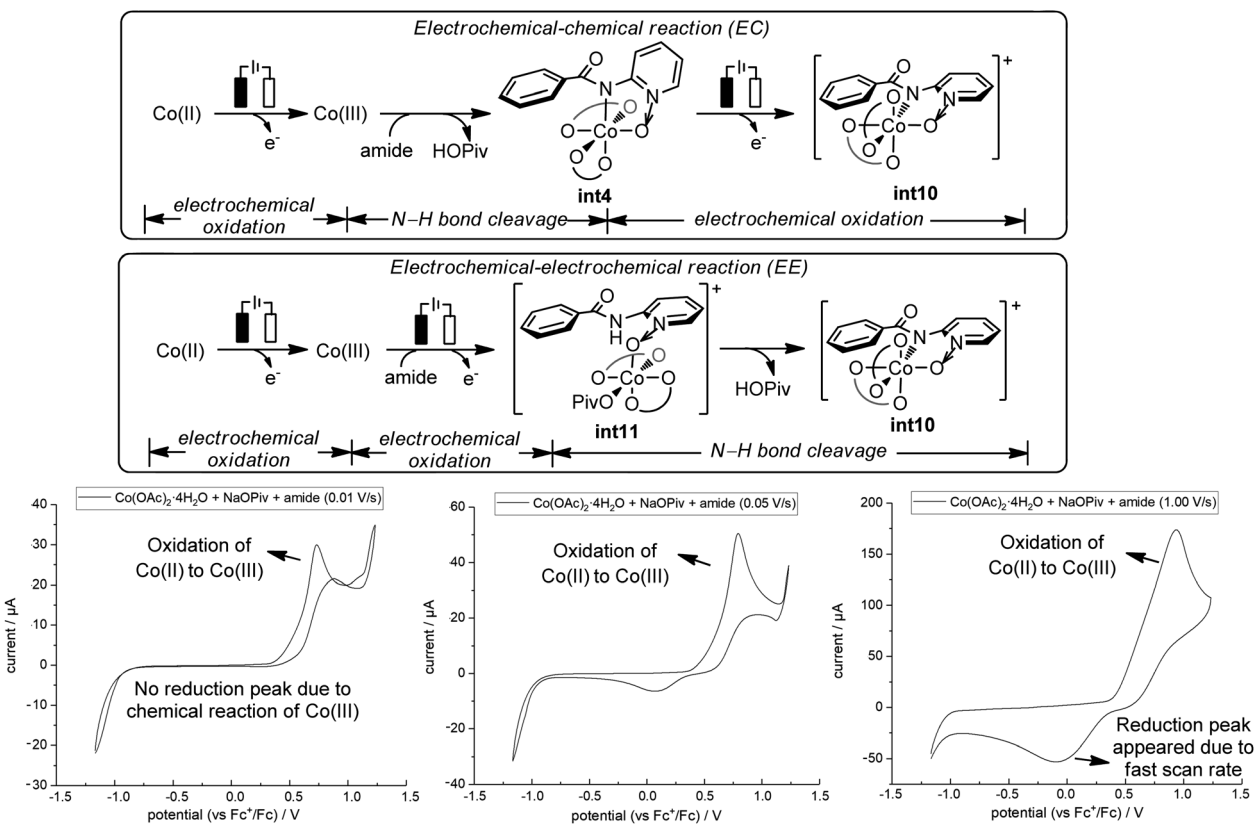

Fig. 2 Cyclic voltammetry studies with varying scan rates. The measurements were carried out at scan rates of 0.01 V s^{-1}, 0.05 V s^{-1}, and 1.00 V s^{-1} respectively in a solvent mixture of DCM and MeOH (4 : 1), with electrolyte *n*-Bu_4NPF_6 (0.05 M). Amide (substrate **1**) (0.5 mM), $NaOPiv \cdot H_2O$ (2 mM), and $Co(OAc)_2 \cdot 4H_2O$ (0.5 mM).

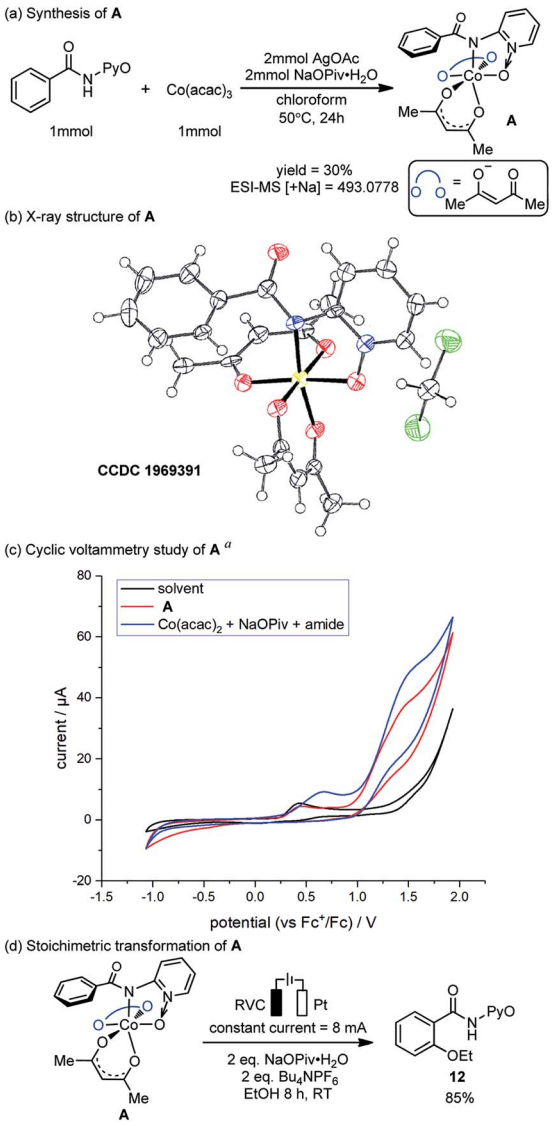

Scheme 3 Synthesis, characterization, cyclic voltammetry study and stoichiometric reaction of amidylcobalt(III) species. [a]The measurements were carried out at a scan rate of 0.10 V s^{-1} in a solvent mixture of DCM and MeOH (4 : 1), with electrolyte *n*-Bu_4NPF_6 (0.05 M). Amide (substrate **1**) (0.5 mM), $NaOPiv \cdot H_2O$ (2 mM), and $Co(acac)_2$ (0.5 mM).

structure of **A** was unambiguously determined by X-ray diffraction (Scheme 3b). Additional NMR and UV-Vis characterization of **A** is included in the ESI.† The CV study of the amidylcobalt(III) species **A** is shown in Scheme 3c (red curve). The oxidation peak of **A** matched well with the second oxidation peak of the reaction mixture involving the amide substrate **1**, $Co(acac)_2$ and $NaOPiv \cdot H_2O$. This further supports the mechanistic proposal that the second electro-oxidation occurs on the amidylcobalt(III) intermediate with the arene C–H bonds being intact. **A** is stable in basic solution without additional oxidants (Scheme S3†). This is consistent with the above calculations that the Co(III)-mediated C–O bond formation is unfeasible (Fig. 1). Under electro-oxidizing conditions, **A** is smoothly transformed into the oxygenation product **12** (Scheme 3d). This corroborated the mechanistic proposal that a second on-cycle electro-oxidation is necessary for C–O bond formation. It should be noted that the chemical oxidation with Ag_2O also allowed the desired oxygenation of **A** to occur (Scheme S4†), which suggests that the amidylcobalt(IV) intermediate could be involved in both electro-chemical and chemical oxidation processes.

We next investigated the mechanistic pathway from the formal Co(IV) intermediate, and the DFT-computed free energy changes are included in Fig. 3. A complexation of **int10** with the pivalate anion leads to the neutral intermediate **int13**. This intermediate undergoes a carboxylate-assisted HAT process to cleave the arene C–H bond *via* **TS14** (*vide infra*), generating a high-energy intermediate **int15** with a phenyl radical. The alternative proton transfer process for the arene C–H bond cleavage is much less favorable (Fig. S8†), and the CMD transition state cannot be located despite extensive efforts. The phenyl radical of **int15** is intramolecularly trapped by cobalt to form the arylcobalt intermediate **int16**. This exergonic cobalt–aryl bond formation compensates the endergonicity of the HAT step. From **int16**, the coordinating pivalic acid dissociates to generate **int17**. Subsequently, methanol complexes through hydrogen-bonding in **int18**, and the C–O bond formation proceeds *via* **TS19**. This C–O bond formation only requires a barrier of 16.0 kcal mol^{-1} and is significantly more efficient than the corresponding process *via* **TS8** (Fig. 1). Information on further exergonic proto-demetalation, additional spin states, and IRC confirmations of each transition state are included in the ESI (Fig. S9–S12†).

The nature of hydrogen-atom-transfer of the carboxylate-assisted C–H bond activation was further characterized by the natural spin density distribution (Fig. 4). In the doublet **int13**, the radical spin is mainly located in O^1, N and O^2. The radical character of the pivalate oxygen O^1 allows the hydrogen-atom-transfer though **TS14**, and a significant radical distribution exists on the forming phenyl radical in this transition state. The overall hydrogen-atom-transfer produces the phenyl radical in **int15**, and the spin density is now mainly distributed in the carbon radical atom. This change of spin distribution is consistent with previous theoretical studies on HAT,[13] and our computational Hammett analysis also confirmed that the radical-stabilizing substituents can facilitate this HAT process (Scheme S1†).[14]

We want to emphasize that the radical character of the coordinating pivalate is crucial for the HAT mechanism. Pivalate is generally considered as a basic and anionic ligand instead of a radical ligand. This is why the carboxylate-assisted arene C–H bond activation generally proceeds *via* a concerted-metalation-deprotonation mechanism in which the hydrogen transfers as a proton.[7c,g] In the electro-oxidized formal Co(IV) intermediate **int13**, considerable radical distribution exists on the coordinating heteroatoms (Fig. 4). This allows the coordinating pivalate to behave as a radical-type hydrogen atom acceptor, leading to the HAT mechanism for arene C–H bond cleavage.

The mechanistic elucidation indicates that the anodic oxidation is not simply responsible for the regeneration of the active transition metal catalyst at the end of the catalytic cycle,[15]

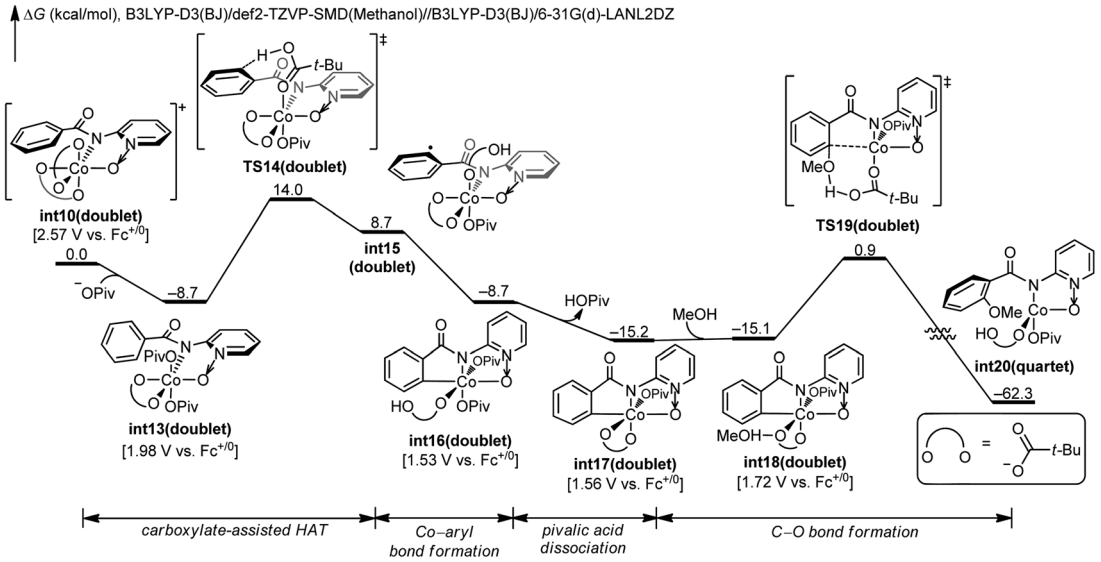

Fig. 3 DFT-computed free energy changes of the pathway from formal Co(IV) intermediate **int10** and computed oxidation potentials of intermediates.

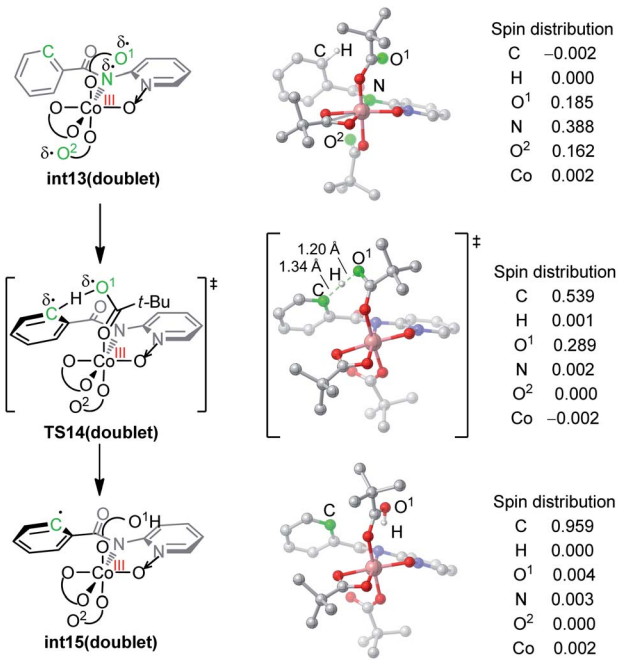

Fig. 4 DFT-optimized structures and the spin density distribution of the C–H activation transition state and intermediates.

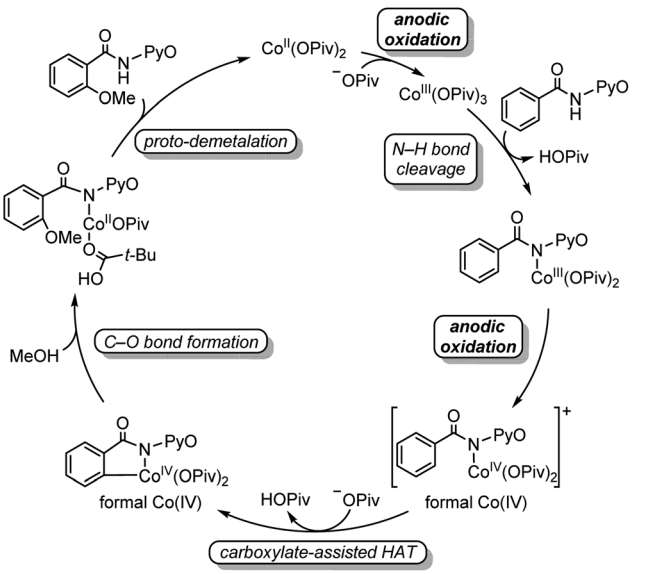

Scheme 4 Overall catalytic cycle of electrochemical cobalt-catalyzed C–H oxygenation.

or the oxidation of an organometallic intermediate to a high-valent species for efficient reductive elimination.[16] In the case of the studied electrochemical cobalt-catalyzed C–H oxygenation with the pyridine-*N*-oxide directing group, the anodic oxidation plays two important roles in transforming cobalt(II) into cobalt(III) and oxidation of the amidylcobalt(III) species to the corresponding formal cobalt(IV) intermediate. These insights emphasized the mechanistic importance of a redox non-innocent ligand[17] in 3d transition metal catalysis, which requires cautious mechanistic proposals. In addition, the change of the directing group may also alter the mechanistic picture, which is currently under investigation in our laboratories. It should be noted that the related C–H activated cyclometallated cobalt(III) species was recently discovered under the electro-oxidative conditions, whose transformations followed the sequence of C–H activation and a following oxidatively induced reductive elimination upon anodic oxidation.[18]

Conclusions

In summary, the potential mechanism of electrochemical cobalt-catalyzed C–H oxygenation was revealed by combined

computational and experimental studies (Scheme 4). An initial electrochemical oxidation generates Co(III) pivalate, and subsequent N–H bond cleavage leads to the amidylcobalt(III) intermediate. This intermediate undergoes a second electrochemical oxidation, which oxidizes the coordinating amidyl fragment to the corresponding radical in the formal Co(IV) intermediate. In the formal Co(IV) intermediate, the radical character of the coordinating carboxylate allows a HAT process to cleave the arene C–H bond. Subsequent C–O bond formation proceeds in a concerted fashion, and the formed amidylcobalt(II) intermediate undergoes a proto-demetalation to release the oxygenated product as well as regenerate the Co(II) catalyst. A Co(II/III/I) catalytic cycle involving a CMD-type mechanism could be excluded by computational studies due to the unfeasible Co(III)-mediated C–O bond formation. This HAT-type C–H bond activation is distinctive from the general CMD mechanism in thermal catalysis, which could provide advantages for C(sp3)–H bond activation. Further studies on the controlling factors of the carboxylate-assisted HAT and mechanism-based design of electrochemical C–H functionalizations are ongoing in our laboratories and will be reported in due course.

Conflicts of interest

There are no conflicts to declare.

Acknowledgements

Financial support from the NSFC (21702182 and 21873081 for X. H. 51771174 for F.-H. C.), DFG (Gottfried-Wilhelm-Leibniz prize) (L. A.), "Fundamental Research Funds for the Central Universities" (2-2050205-19-361 for X. H. and H.-J. X.) and China Postdoctoral Science Foundation (2018M640546 for S.-Q. Z.) is gratefully acknowledged. Calculations were performed on a high-performance computing system at the Department of Chemistry, Zhejiang University.

Notes and references

1 For selected reviews of electrochemical C–H activation, see: (*a*) L. Ackermann, *Acc. Chem. Res.*, 2020, **53**, 84; (*b*) T. H. Meyer, L. H. Finger, P. Gandeepan and L. Ackermann, *Trends in Chemistry*, 2019, **1**, 63; (*c*) Z. Ye and F. Zhang, *Chin. J. Chem.*, 2019, **37**, 51; (*d*) C. Song, K. Liu, X. Dong, C. Chiang and A. Lei, *Synlett*, 2019, **30**, 1149; (*e*) M. Kärkäs, *Chem. Soc. Rev.*, 2018, **47**, 578; (*f*) K. Liu, C. Song and A. Lei, *Org. Biomol. Chem.*, 2018, **16**, 2375; (*g*) S. Tang, Y. Liu and A. Lei, *Chem*, 2018, **4**, 27; (*h*) Q. Yang, P. Fang and T. Mei, *Chin. J. Chem.*, 2018, **36**, 338. For general reviews on organic electrosynthesis see: (*i*) A. Wiebe, T. Gieshoff, S. Möhle, E. Rodrigo, M. Zirbes and S. R. Waldvogel, *Angew. Chem., Int. Ed.*, 2018, **57**, 5594; (*j*) M. Yan, Y. Kawamata and P. Baran, *Chem. Rev.*, 2017, **117**, 13230; (*k*) E. Horn, B. Rosen and P. Baran, *ACS Cent. Sci.*, 2016, **2**, 302; (*l*) R. Francke and R. Little, *Chem. Soc. Rev.*, 2014, **43**, 2492.

2 For selected reviews of electrochemical transition metal-catalyzed C–H functionalization, see: (*a*) H. Wang, X. Gao, Z. Lv, T. Abdelilah and A. Lei, *Chem. Rev.*, 2019, **119**, 6769; (*b*) N. Sauermann, T. H. Meyer, Y. Qiu and L. Ackermann, *ACS Catal.*, 2018, **8**, 7086; (*c*) C. Ma, P. Fang and T. Mei, *ACS Catal.*, 2018, **8**, 7179; (*d*) K. Jiao, C. Zhao, P. Fang and T. Mei, *Tetrahedron Lett.*, 2017, **58**, 797; (*e*) F. Kakiuchi and T. Kochi, *Isr. J. Chem.*, 2017, **57**, 953. For a review on cobalt-catalyzed electrochemical C–H functionalization, see: (*f*) N. Sauermann, T. H. Meyer and L. Ackermann, *Chem.–Eur. J.*, 2018, **24**, 16209.

3 (*a*) C. Tian, U. Dhawa, J. Struwe and L. Ackermann, *Chin. J. Chem.*, 2019, **37**, 552; (*b*) N. Sauermann, T. H. Meyer, C. Tian and L. Ackermann, *J. Am. Chem. Soc.*, 2017, **139**, 18452.

4 (*a*) N. Sauermann, R. Mei and L. Ackermann, *Angew. Chem., Int. Ed.*, 2018, **57**, 5090; (*b*) X. Gao, P. Wang, L. Zeng, S. Tang and A. Lei, *J. Am. Chem. Soc.*, 2018, **140**, 4195.

5 (*a*) R. Mei, W. Ma, Y. Zhang, X. Guo and L. Ackermann, *Org. Lett.*, 2019, **21**, 6534; (*b*) J. Chen, L. Jin, J. Zhou, X. Jiang and C. Yu, *Tetrahedron Lett.*, 2019, **60**, 2054; (*c*) C. Tian, L. Massignan, T. H. Meyer and L. Ackermann, *Angew. Chem., Int. Ed.*, 2018, **57**, 2383; (*d*) R. Mei, N. Sauermann, C. Joao, A. Oliveira and L. Ackermann, *J. Am. Chem. Soc.*, 2018, **140**, 7913; (*e*) T. H. Meyer, J. C. A. Oliveira, S. Sau, N. Ang and L. Ackermann, *ACS Catal.*, 2018, **8**, 9140; (*f*) S. Tang, D. Wang, Y. Liu, L. Zeng and A. Lei, *Nat. Commun.*, 2018, **9**, 798.

6 (*a*) S. Sau, R. Mei, J. Struwe and L. Ackermann, *ChemSusChem*, 2019, **12**, 1; (*b*) L. Zeng, H. Li, S. Tang, X. Gao, Y. Deng, G. Zhang, C. Pao, J. Chen, J. Lee and A. Lei, *ACS Catal.*, 2018, **8**, 5448.

7 For selected reviews of mechanistic studies on transition metal-catalyzed C–H bond activation, see: (*a*) X. Qi, Y. Li, R. Bai and Y. Lan, *Acc. Chem. Res.*, 2017, **50**, 2799; (*b*) Y. Yang, X. Hong, J. Yu and K. N. Houk, *Acc. Chem. Res.*, 2017, **50**, 2853; (*c*) D. Davies, S. Macgregor and C. McMullin, *Chem. Rev.*, 2017, **117**, 8649; (*d*) X. Zhang, L. Chung and T. Wu, *Acc. Chem. Res.*, 2016, **49**, 1302; (*e*) T. Sperger, I. Sanhueza, I. Kalvet and F. Schoenebeck, *Chem. Rev.*, 2015, **115**, 9532; (*f*) D. Musaev, T. Figg and A. Kaledin, *Chem. Soc. Rev.*, 2014, **43**, 5009; (*g*) L. Ackermann, *Chem. Rev.*, 2011, **111**, 1315; (*h*) T. Lyons and M. Sanford, *Chem. Rev.*, 2010, **110**, 1147.

8 For a review on mechanistic studies of electrochemical transition-metal catalysis, see: A. Jutand, *Chem. Rev.*, 2008, **108**, 2300.

9 For selected mechanistic studies on cobalt-catalyzed C–H bond activation, see: (*a*) P. Ma and H. Chen, *ACS Catal.*, 2019, **9**, 1962; (*b*) Y. W. C. Du, Y. Wang, X. Guo, L. Fang, M. Song, J. Niu and D. Wei, *Adv. Synth. Catal.*, 2018, **360**, 2668; (*c*) M. Li and J. Wang, *Org. Lett.*, 2018, **20**, 6490; (*d*) R. Mei, H. Wang, S. Warratz, S. Macgregor and L. Ackermann, *Chem.–Eur. J.*, 2016, **22**, 6759; (*e*) S. Maity, R. Kancherla, U. Dhawa, E. Hoque, S. Pimparpar and D. Maiti, *ACS Catal.*, 2016, **6**, 5493; (*f*) O. Planas, C. Whiteoak, V. Martin-Diaconescu, I. Gamba, J. Luis,

T. Parella, A. Company and X. Ribas, *J. Am. Chem. Soc.*, 2016, **138**, 14388; (*g*) X. Guo, L. Zhang, D. Wei and J. Niu, *Chem. Sci.*, 2015, **6**, 7059.

10 Computations are performed with the Gaussian 09 program, reference: Frisch, M. J., et al., Gaussian 09, revision C.01; Gaussian Inc., Wallingford, CT, 2016, Computational details are provided in the ESI.†

11 (*a*) A. Bard and L. Faulkner, *Electrochemical Methods Fundamentals and Applications*, John Wiley & Sons, 2001; (*b*) For a recent study involving mechanistic understading of electrochemical organic synthesis, see: B. Peters, K. Rodriguez, S. Reisberg, S. Beil, D. Hickey, Y. Kawamata, M. Collins, J. Starr, L. Chen, S. Udyavara, K. Klunder, T. Gorey, S. Anderson, M. Neurock, S. Minteer and P. S. Baran, *Science*, 2019, **363**, 838.

12 The CV studies on individual species confirmed the oxidation potential of Co(II), details are included in the ESI (Fig. S15†).

13 (*a*) J. Li, S. Zhou, J. Zhang, M. Schlangen, T. Weiske, D. Usharani, S. Shaik and H. Schwarz, *J. Am. Chem. Soc.*, 2016, **138**, 7973; (*b*) J. Li, S. Zhou, J. Zhang, M. Schlangen, D. Usharani, S. Shaik and H. Schwarz, *J. Am. Chem. Soc.*, 2016, **138**, 11368; (*c*) H. Schwarz, *Chem. Phys. Lett.*, 2015, **629**, 91.

14 For a consistent Hammett analysis of the HAT process, see: J. Paulo, T. Zaragoza, M. Siegler and D. Goldberg, *J. Am. Chem. Soc.*, 2018, **140**, 4380.

15 (*a*) Y. Qiu, A. Scheremetjew and L. Ackermann, *J. Am. Chem. Soc.*, 2019, **141**, 2731; (*b*) Q. Yang, Y. Xing, X. Wang, H. Ma, X. Weng, X. Yang, H. Guo and T. Mei, *J. Am. Chem. Soc.*, 2019, **141**, 18970; (*c*) T. Koyanagi, A. Herath, A. Chong, M. Ratnikov, A. Valiere, J. Chang, V. Molteni and J. Loren, *Org. Lett.*, 2019, **21**, 816; (*d*) X. Gao, P. Wang, L. Zeng, S. Tang and A. Lei, *J. Am. Chem. Soc.*, 2018, **140**, 4195; (*e*) Y. Qiu, W. Kong, J. Struwe, N. Sauermann, T. Rogge, A. Scheremetjew and L. Akermann, *Angew. Chem., Int. Ed.*, 2018, **57**, 5828.

16 (*a*) A. Shrestha, M. Lee, A. Dunn and M. Sanford, *Org. Lett.*, 2018, **20**, 204; (*b*) S. Zhang, R. Samanta, N. Sauermann and L. Ackermann, *Chem.–Eur. J.*, 2018, **24**, 19166; (*c*) Y. Li, Q. Yang, P. Fang, T. Mei and D. Zhang, *Org. Lett.*, 2017, **19**, 2905; (*d*) C. Ma, C. Zhao, Y. Li, L. Zhang, X. Xu, K. Zhang and T. Mei, *Chem. Commun.*, 2017, **53**, 12189; (*e*) Q. Yang, Y. Li, C. Ma, P. Fang, X. Zhang and T. Mei, *J. Am. Chem. Soc.*, 2017, **139**, 3293.

17 For selected reviews of redox non-innocent ligands, see: (*a*) J. I. Vlugt, *Chem.–Eur. J.*, 2019, **25**, 2651; (*b*) V. Lyaskovskyy and B. Bruin, *ACS Catal.*, 2012, **2**, 270.

18 T. H. Meyer, J. C. A. Oliveira, D. Ghorai and L. Ackermann, *Angew. Chem., Int. Ed.*, 2020, **59**, 1.

